The birth of a dinosaur footprint: Subsurface 3D motion reconstruction and discrete element simulation reveal track ontogeny

Peter L. Falkingham[a,b,1] and Stephen M. Gatesy[b]

[a]Structure and Motion Laboratory, Department of Comparative Biomedical Sciences, Royal Veterinary College, Hatfield AL97TA, United Kingdom; and [b]Department of Ecology and Evolutionary Biology, Brown University, Providence, RI 02912

Edited by Neil H. Shubin, The University of Chicago, Chicago, IL, and approved October 30, 2014 (received for review August 22, 2014)

Locomotion over deformable substrates is a common occurrence in nature. Footprints represent sedimentary distortions that provide anatomical, functional, and behavioral insights into trackmaker biology. The interpretation of such evidence can be challenging, however, particularly for fossil tracks recovered at bedding planes below the originally exposed surface. Even in living animals, the complex dynamics that give rise to footprint morphology are obscured by both foot and sediment opacity, which conceals animal–substrate and substrate–substrate interactions. We used X-ray reconstruction of moving morphology (XROMM) to image and animate the hind limb skeleton of a chicken-like bird traversing a dry, granular material. Foot movement differed significantly from walking on solid ground; the longest toe penetrated to a depth of ∼5 cm, reaching an angle of 30° below horizontal before slipping backward on withdrawal. The 3D kinematic data were integrated into a validated substrate simulation using the discrete element method (DEM) to create a quantitative model of limb-induced substrate deformation. Simulation revealed that despite sediment collapse yielding poor quality tracks at the air–substrate interface, subsurface displacements maintain a high level of organization owing to grain–grain support. Splitting the substrate volume along "virtual bedding planes" exposed prints that more closely resembled the foot and could easily be mistaken for shallow tracks. DEM data elucidate how highly localized deformations associated with foot entry and exit generate specific features in the final tracks, a temporal sequence that we term "track ontogeny." This combination of methodologies fosters a synthesis between the surface/layer-based perspective prevalent in paleontology and the particle/volume-based perspective essential for a mechanistic understanding of sediment redistribution during track formation.

footprint | dinosaur | locomotion | discrete element method | XROMM

Terrestrial locomotion is vital to the survival of many vertebrate animals, and is expressed in typical behaviors such as food acquisition, predator avoidance, mate finding, and population dispersal. Generalized models of legged movement are typically derived from laboratory studies of walking and running on stiff, solid surfaces; however, locomotion over compliant, yielding substrates is also important, for two reasons. First, animals frequently encounter such terrain—unconsolidated desert sand, river banks, shorelines, snow, or simply soil after rain—in their natural environments. Movement over such deformable substrates is, accordingly, a major research area in biomechanics and robotics (1–3). Second, feet that deform malleable substrates leave tracks. Footprints can be a major source of information about an animal or group of animals (4–6), and this is particularly true for extinct taxa that cannot be observed directly (7–9). Indeed, the only movements that have been recorded in the fossil record were necessarily over/through suitably compliant substrates (10).

Despite tracks being so common and holding so much potential, extracting reliable inferences from a footprint's final morphology is rarely straightforward. A track is not a simple mold of static pedal anatomy, but rather the end product of a dynamic sequence of interactions between the moving foot and substrate (11–14). Even data collected by direct observation of track formation is incomplete and frustratingly elusive. Because sinking of the foot is intrinsic to the process, motions of the distal limb, the limb–substrate interface, and all subsurface sediment remain hidden from view.

Several previous studies have focused on describing deformation at deeper levels to interpret fossil tracks exposed at bedding planes beneath the surface on which the animal walked. Experimental tracks have been created predominantly in horizontal layers of colored material that were later sectioned or split apart (15–19). Such destructive methods lack a temporal component, precluding direct association of individual track features with specific anatomical structures and explicit events in the step cycle. Recent work using two X-ray systems (20) noninvasively documented the 3D path of radiopaque sediment markers throughout track formation; however, this approach suffers from artificial indenter motion and limited spatial resolution.

Herein we describe results of a study in which we recorded live birds traversing granular and solid substrates with biplanar X-ray video. The 3D motion of the hind limb bones was reconstructed, both above and below the substrate surface. These skeletal kinematics were then incorporated into a validated computer simulation of the substrate to visualize subsurface sediment deformation. Exploration of the simulated volume over time offers a dynamic glimpse into the previously invisible process of track formation, which we term "track ontogeny."

Results

Three-Dimensional Foot and Limb Kinematics. The guineafowl walked steadily over both a solid platform and a trough of poppy

Significance

We reconstructed the 3D foot movements of guineafowl traversing a granular substrate from biplanar X-rays, and then incorporated those kinematics into a discrete element simulation. Digital track models permitted visualization of in vivo track formation at the surface and at virtual bedding planes for the first time. Application of these volumetric data to fossil dinosaur tracks uncovered the developmental origin of previously enigmatic features. A "track ontogeny" perspective helps integrate limb and substrate dynamics into the interpretation of track morphology, from which foot anatomy cannot be read directly.

Author contributions: P.L.F. and S.M.G. designed research, performed research, analyzed data, and wrote the paper.

The authors declare no conflict of interest.

This article is a PNAS Direct Submission.

[1]To whom correspondence should be addressed. email: pfalkingham@rvc.ac.uk.

This article contains supporting information online at www.pnas.org/lookup/suppl/doi:10.1073/pnas.1416252111/-/DCSupplemental.

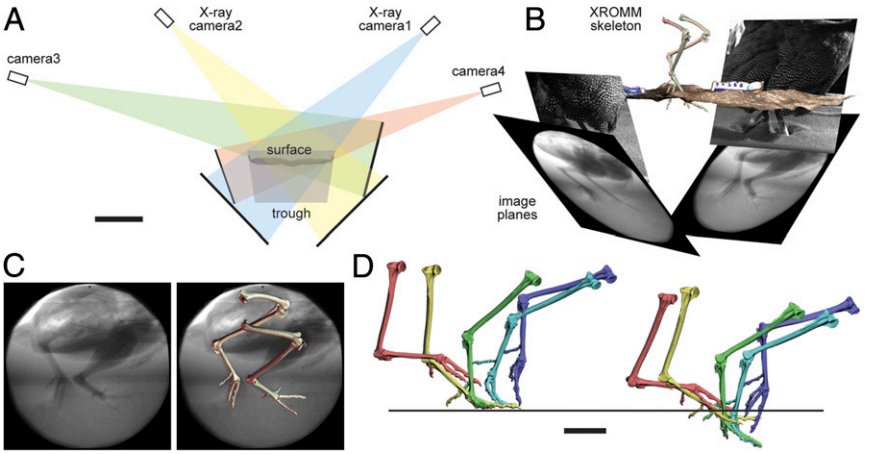

Fig. 1. XROMM analysis of guineafowl limb movement through a compliant substrate (poppy seeds). (*A*) End view of the sediment trackway, showing the volume covered by the two X-ray beams (blue and yellow), and the two calibrated light cameras (red and green). The intersection of the X-ray beams continues below the sediment surface. (*B*) Perspective view of the Maya scene showing the four image planes, the reconstructed skeletal model, and the photogrammetric model of the tracks. (*C*) Frame of the X-ray video showing subsurface imaging and the registered bone models. (*D*) Comparison of steps on solid (*Left*) and dry, granular (*Right*) substrates for the same individual. (Scale bars: 20 cm in *A*; 5 cm in *D*.)

seeds. The biplanar X-ray volume was large enough to allow reconstruction of 3D motions of the limb skeleton from the knee down throughout one step by X-ray reconstruction of moving morphology (XROMM) (Fig. 1 *A*–*C* and Movie S1). We identified comparable stages of the locomotor cycle based on motion of the tarsometatarsus (Fig. 1*D*), and distinguished major differences in kinematic patterns between substrates.

On the solid platform, the knee remained 16–18 cm above the surface during the stance phase. Soon after contact with the platform, the three forward-facing toes (digits II–IV) came to lie horizontally along most of their length. Later in stance phase, these toes rolled smoothly up and forward, sequentially lifting from proximal to distal. The longest toe (digit III) pivoted about the tip of its claw, cleanly transitioning into swing phase without slipping backward.

On poppy seeds, the foot immediately plunged beneath the sediment on contact. Penetration lowered knee height, which varied from only 12 cm to 15 cm above the level of the undisturbed surface. Differences with the motion pattern used on the platform were most dramatic in the submerged toes. Digits II–IV initially penetrated ~1 cm while remaining parallel to the surface, but subsequently descended claws-first until oriented ~30° below horizontal. The tip of digit III reached a depth of ~5 cm and was swept backward and upward on withdrawal.

Physical and Simulated Track Morphology. Guineafowl walking through poppy seeds produced a linear series of oblong depressions bordered anteriorly by raised rims (Fig. 2 *A*, *C*, and *D*). A vaguely cruciform pattern of grooves was sometimes discernible within each track; however, distinct digit impressions were lacking. Using XROMM-derived foot movement, the discrete element method (DEM) model produced a simulated surface track closely corresponding to the physical tracks (Fig. 2 *B* and *E* and Movie S2). An exact match was not expected; the bird's right and left tracks overlapped and were formed on an uneven surface, whereas a single track was simulated in the initially smooth DEM volume.

Unlike the opaque poppy seeds, the model allows visualization of displacement of subsurface material. By segregating particles according to their initial height, we can designate horizontal "layers" in the homogeneous substrate and follow their fate. Five samplings of the simulated data at 1-cm depth increments revealed the dynamic effects of locomotion on the sediment volume (Fig. 3 and Fig. S1). When particles belonging to originally higher layers are rendered invisible, a footprint is revealed that is analogous to one exposed by splitting along a bedding plane in fossilized sediments. Transitional and final track contours are clearly shown on color height maps. Warm-colored particles are elevated above each green "virtual bedding plane," whereas cool-colored particles are exposed lying below these planes.

Final track morphology varied dramatically with depth (Fig. 3*E*). The most striking difference was the definition of uppermost and deeper surfaces. Unlike the collapsed air-sediment boundary, sediment–sediment interfaces below approximately 1 cm clearly recorded the passage of the foot. Toe impressions were preserved as deep, steep-walled incisions. Tracks at a depth of 1–2 cm also showed obvious uplifted features formed from particles that rose well above their original starting depth. At 3 cm, a very faint trace of the hallux (digit I) was discerned, but at this and deeper bedding planes, the tracks are reduced to depressions left by the distal tips of digits II–IV.

Simulation provides temporal information as well, revealing intermediate stages in the development of each track (Fig. 3 *A*–*D*).

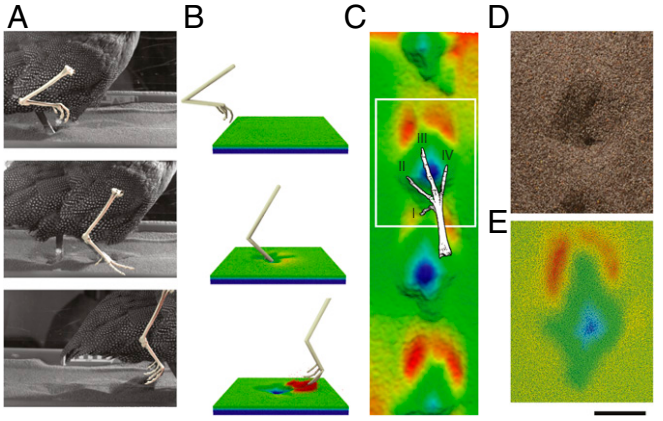

Fig. 2. Simulation of a guineafowl track. (*A* and *B*) Sequence of three video frames with registered bone models (*A*) and their virtual counterparts (*B*). (*C*) Colored height map of real tracked surface, indicating the location of the foot at touchdown. (*D*) Photograph of the track analyzed (white box in *C*). (*E*) Height map of the discrete element model, simulated from the kinematics associated with the track shown in *D* (white box in *C*). (Scale bar: 5 cm.)

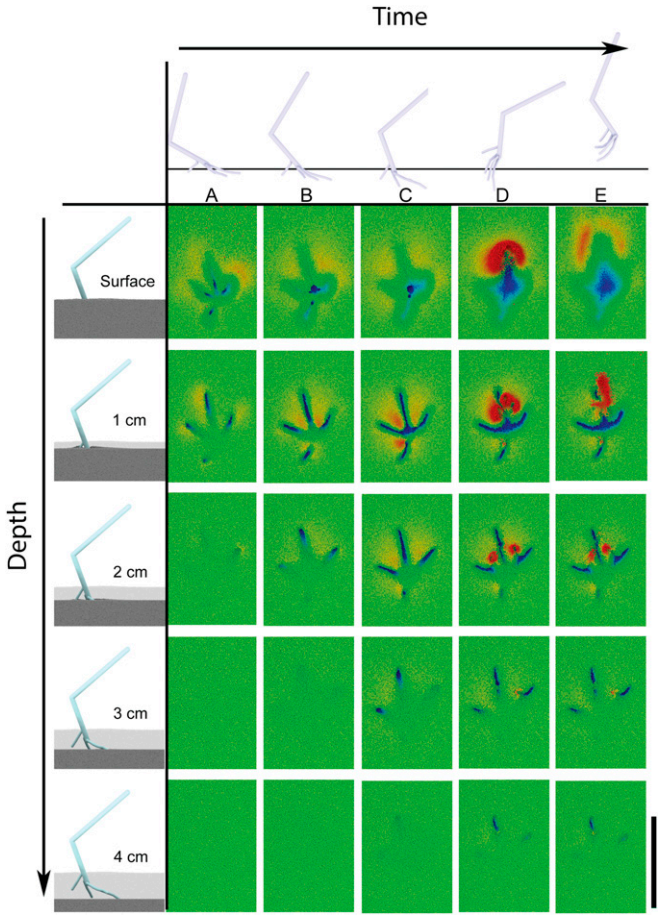

Fig. 3. Track ontogeny. Simulated track using the motions of guineafowl traversing poppy seeds as part of a discrete element simulation. Each virtual bedding plane within the sediment volume is exposed by reducing the opacity of initially overlying grains. (Scale bar: 10 cm.)

The uppermost fraction of the sediment volume underwent constant changes as particles reacted to the entry/exit of the toes and tarsometatarsus, as well as to gravity. During foot penetration, particles were moved downward and to a lesser extent forward; however, the leading zone of deformation was quite thin (~5–6 mm). Clear tracks resembling the toe tips were not transmitted far in advance of the descending skin–sediment interface, leaving the 4-cm horizon undeformed until very late in the step cycle. The descending foot also displaces particles upward (Fig. 3 *A*–*C*), with additional material drawn even higher on withdrawal (Fig. 3 *D* and *E*).

Discussion

In this study, we image and reconstruct in 3D the subsurface movement of a bird's foot as it traversed dry poppy seeds. Guineafowl walking on this compliant substrate not only sink below the surface, but also use toe kinematics distinct from those used on solid ground. By incorporating XROMM-based motion into a DEM simulation, the poppy seed volume was modeled as particles that could be traced throughout their complex reconfiguration. The combination of simulation with in vivo kinematics provides a first glimpse at the temporal sequence of foot–substrate and substrate–substrate interactions giving rise to final track morphology. Just as developmental biologists seek to understand the changes taking place from zygote to adult during the life of an individual (21), we wish to illuminate the origin and modification of specific features throughout track ontogeny. Such dynamic insight provides a more robust context for interpreting the footprints of dinosaurs and other taxa in the fossil record, particularly those today exposed at former subsurface bedding planes.

Track Formation in Dry, Granular Media. Near the sediment–air interface, poppy seeds are relatively unconstrained and able to move rather freely. Weak grain–grain support causes any high topography to quickly collapse to the angle of repose (~30°), leaving indistinct surface tracks that lack definition (Fig. 2 *C* and *D*). Observed in isolation, the inference of digit number, interdigital angle, or even approximate size of the track maker's foot, would be difficult to make with any confidence from such evidence. The faint cruciform creases lie well above the lowest point reached by each digit, and so do not represent toe impressions in the conventional sense. Rather, the rear and side indentations mark the entry of digits I, II, and IV into the substrate. Loose grains falling into the depressions quickly cover the descending toes and obscure any details of anatomy or movement. Digit III is buried similarly, but its entry groove is transient and subsequently reworked as the foot is withdrawn from the substrate. The large front furrow seen in the final track arises through rotation of the tarsometatarsus and the emergence of all four, converged toes upon withdrawal (Fig. 2 *A* and *B*).

Unlike at the sediment–air interface, exposure along virtual bedding planes reveals well-defined features below the surface (Fig. 3*E*). At depth, support from neighboring particles allows sharp edges and steep contours to persist that would immediately collapse near the top of the volume. Overlying material constrains grain movement, thereby fostering the persistence of layers, rather than complete loss of organization, as the foot passes through. Although it may seem counterintuitive, high-definition tracks can be formed, and potentially preserved, even in loose, homogeneous, granular media. This phenomenon can be observed in fossil tracks formed in dune sands and exposed in cross-section (22–24), where laminations are preserved as tightly nested incisions. Above these nested surfaces, sediment loses coherent structure where the lack of grain–grain support has led to collapse. Despite lacking surface tracks with obvious anatomical structure, sediments like dry sand should not be dismissed as poor track-bearing strata.

An Ontogenetic Perspective on Track Morphology. Because the articulated digits interact with the sediment dynamically and obliquely, no initially horizontal surface can be read directly as an exact record of foot anatomy. Taking into account the temporal sequence of foot movements through the volume offers clarification, however; for example, the track created 1 cm below the original surface (Fig. 3*E*) bears impressions of digits II and IV that appear to curve anteriorly. By following the development of the track at this depth (Fig. 3 *A*–*E*), the initially straight depressions made by the penetrating side toes are seen to gradually lose their acute angle and become rounded. Thus, curvature arises from subsequent motion of the digits and tarsometatarsus, not because of any anatomical arc of the toes themselves.

The track formed 2 cm beneath the surface (the approximate maximum depth of tarsometatarsal penetration) resembles pedal morphology most closely (Fig. 3*E*). However, any strict anatomical fidelity is negated by elevated topography that has no homolog in the static foot. Such raised structures in upper surfaces are exit features left by the removal of the digits (warm colors in Fig. 3 *D* and *E*). The side toes remain widely spread throughout penetration, but converge upon withdrawal. As the adducting digits are extracted, particles are driven upward as well, creating raised cones along their path through previously undeformed material. Individual toes thus can impact the same surface twice. At 1 cm depth, blue depressions record the descent of digits II and IV, whereas warm colors mark their ascent.

Once the digits and tarsometatarsus finally emerge into air at the front of the track, particles brought forward and up subsequently collapse into an indistinct raised rim (Fig. 2 *A* and *B*).

Features formed during withdrawal can deform or even obliterate those generated during foot entry, making a direct reading of anatomy from such a track extremely difficult. For example, digit III creates a relatively straight depression at 1 cm depth on its way down (Fig. 3 *A*–*C*). Only later do the converging toes draw particles upward and toward the midline, distorting the originally linear impression into a sinuous curve. This complex ontogenetic sequence shows that in the final track, the S-shaped mark attributed to the third toe arose not by simple stamping, but through the cumulative influence of entry and exit of multiple digits.

Significance for Interpreting Fossil Tracks. At best, a fossil track only records the final sediment conformation at the end of its developmental sequence. Thus, the dynamic origin of features comprising footprint topography must be inferred to correctly reconstruct trackmaker anatomy, limb movement, and substrate properties (9, 25, 26). Combining DEM simulation with accurate 3D foot motion enables the explicit association of topographic features with motions of the foot and sediment throughout the substrate volume. Such ontogenetic data serve as valuable reference for illuminating the significance of ancient track morphology.

As an example, we considered a specimen of *Corvipes lacertoideus* from the Early Jurassic of the Connecticut Valley (Fig. 4*A*). The uppermost track surface bears a trio of raised, semicircular features (white arrows) midway along the S-shaped impression of digit III. Our guineafowl data at a depth of 1 cm show comparable contours in the same location (Fig. 4*B*, warm colors), allowing us to identify these as exit features that distorted the impression of digit III in an equivalent manner. Other specimens of various sizes and ages described globally (26–28) bear similar unexplained topography. Thus, we are able to link specific features of fossil dinosaur tracks to homologous features created by guineafowl ~200 million years later, despite differences in foot anatomy, limb movement, and substrate.

Isolated track surfaces are prone to misinterpretation without volumetric context. A foot directly affects sediment continuously from the surface to its maximum penetration depth, and ancient tracks may be sampled throughout this spectrum. If found in the fossil record, a guineafowl track or trackway from the uppermost surface (Figs. 2 *C* and *D* and 3*E*, surface) could be misidentified either as heavily eroded or as marks left by a very different animal. On discovering a fossilized version of a deeper track (3 cm; Fig. 3*E*), one might reasonably assume it to be the original surface the animal walked on, and that the foot encountered a firm substrate and so sank very little. Errors of this kind may be quite common, prompting the literal interpretation of data such as toe impression length, width, and angle as accurate reflections of pedal anatomy. Such foot-like tracks also pose problems for temporal interpretation at sites where animals deform a surface by penetrating overlying layers at different, and thus noncontemporaneous, stages of sedimentation. The identification and location of exit features, such as described above, may prove valuable for deciphering the relative position of tracks within a sediment volume, although further research is required.

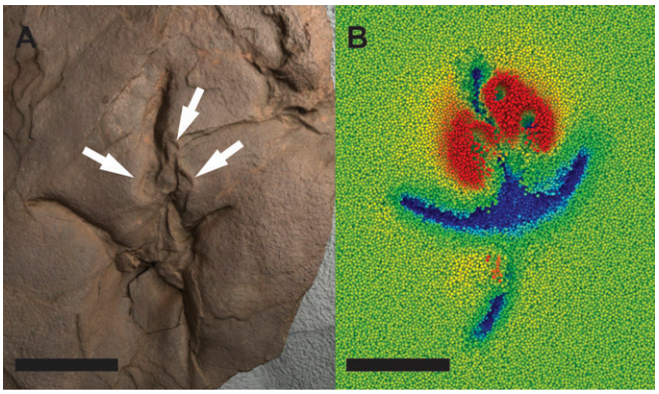

Fig. 4. (*A*) Fossil dinosaur track from the Beneski Museum of Natural History, Amherst College (specimen no. ACM-ICH 37/24; Lower Jurassic). (*B*) Simulated track exposed at 2 cm below the original sediment–air interface. Both tracks display rounded features associated with the withdrawal of the foot, and a sinuosity to the impression of digit III. (Scale bar: 3 cm.)

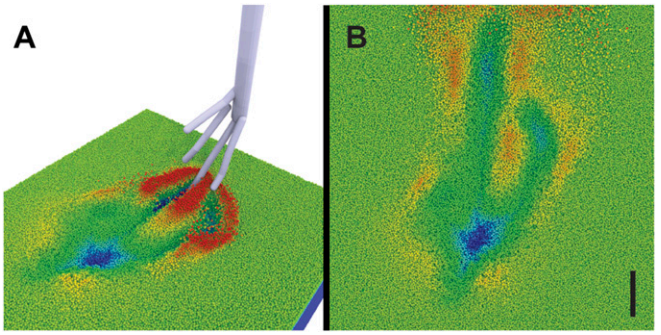

Fig. 5. Simulated track using kinematics captured from a guineafowl walking on a solid surface. (*A*) Perspective view late in withdrawal. (*B*) Top view of the track surface. (Scale bar: 2 cm.)

Using Simulation to Explore the Origins of Track Diversity. The morphology of any track is determined by the interaction between foot anatomy, limb dynamics, and substrate (9, 29, 30). Although this concept is widely accepted in the literature, how the complex interplay between these factors generates track diversity remains poorly understood.

Unlike in living animals, in which anatomy is fixed and motion–substrate interactions are coupled, our virtual environment enables exploration of track determinants independently. For example, what happens when only foot movement is altered? We transferred solid surface walking kinematics into the poppy seed simulation, allowing the tarsometatarsus to sink 2 cm as before. The resultant track, which appears superficially didactyl (Fig. 5), is dramatically different (Figs. 2 and 3), because digits III and IV of the medially angled foot leave elongate scours. This simple test confirms that the simulation is not destined to produce a given track morphology, providing further confidence in the poppy seed model. More importantly, it highlights the significance of dynamic factors in translating foot anatomy into the sedimentary deformation we call tracks. The implications for trackmaker identification and ichnotaxonomy are complex, and will be discussed at length elsewhere.

To move beyond dry, granular materials, XROMM analyses of birds walking through wet, cohesive sediment of varying consistency would quantify kinematic adaptations to a wider range of properties. Validated DEM models of various fine-grained muds would then offer the opportunity to simulate guineafowl sequences for the most common track-bearing substrates in the fossil record. Future simulations will afford the manipulation of multiple factors. Hypotheses of fossil formation could be tested by modifying foot models to have more primitive dinosaur anatomy (e.g., hallux orientation, metatarsal fusion, interdigital angle), and foot kinematics could then be iteratively animated to improve the match between simulated and real fossil tracks.

Our analysis reveals how bedding plane depth (Fig. 3) and relatively subtle kinematic differences (Fig. 1*D*) can result in widely differing track morphologies (Figs. 2*D* and 5). We hope to

use this approach to gain a mechanistic understanding of the origin of track diversity throughout the Mesozoic. Such extant disparity also supports efforts to reconstruct foot motions from fossil tracks, particularly in specimens preserved at multiple levels. An experimental and simulation-based understanding of track ontogeny holds promise for releasing the full potential of fossil tracks to elucidate the evolution of dinosaur locomotion.

Conclusions

The combination of XROMM and DEM methodologies fosters a mechanistic understanding of sediment redistribution during track formation. The methods enable visualization through not only depth, but also time, an aspect we term track ontogeny. Observable track morphology is the final product of this ontogeny, and should be interpreted in light of this, given that features formed on foot entry can be distorted or destroyed as the foot is withdrawn.

Materials and Methods

XROMM Data Capture and Analysis of Birds Traversing Loose Substrate. Our experimental setup was as described previously (31). Helmeted guineafowl (*Numida meleagris* L.) were obtained from a local breeder for this study. Animals were housed at Brown University's Animal Care Facility with unlimited access to food and water. Data were collected from multiple individuals as part of a larger study, but here we present representative data from a single bird. All experiments using animals were carried out in accordance with Brown University's Institutional Animal Care and Use Committee.

A 3.75-m-long walkway was constructed at Brown University in the W. M. Keck Foundation XROMM Facility. The center section of the trackway consisted of a plastic trough 20 cm deep, 30 cm wide, and 125 cm long, filled to a depth of ∼18 cm with dry poppy (*Papaver somniferum*) seeds 1 mm in diameter. Covered pet carriers were placed at each end of the trackway to provide refuge for the birds, which were restricted from escaping by clear acrylic walls when walking through the sediment. Poppy seeds were used as a compliant substrate because they behave qualitatively like dry sand (1), but have a much lower radiopacity, allowing X-ray imaging of guineafowl phalanges.

The sediment trough was situated at the intersection of two X-ray beams (configured at 45° from vertical), such that synchronized high-resolution (1,760 × 1,760), high-speed (250 fps) video of footfalls could be recorded with Photron high-speed cameras. Two additional synchronized Photron cameras recorded standard light video (1,600 × 1,200, 250 fps) above the surface in the same area (Fig. 1). Locomotion on a solid surface was recorded from the same birds in the same experimental setup by placing a composite panel (carbon fiber with foam core) over the trough to form a solid platform. Videos were processed in MATLAB (MathWorks) using the X-rayProject suite (32), and then imported, with calculated camera positions, into Autodesk Maya.

A computed tomography (CT) scan of the bird was segmented into individual bones using 3D Slicer (www.slicer.org). These bone models were then imported into Maya and rigged such that translation and rotation of the entire limb was controlled from the tarsometatarsus (TMT). Individual phalanges were rigged to the TMT using a series of joints placed at the centroid of the preceding condyles, and the tibia was rigged so as to be rotated from the ankle joint. The bones were then rotoscoped to the X-ray videos in Maya through scientific rotoscoping (33–35) to produce a digital reconstruction of the 3D kinematics of the limb above and below the surface of the substrate throughout the duration of the step cycle.

All calibration images, raw videos, and CT files were uploaded to the XMA Portal, a web-based environment for storage, management, and sharing of XROMM data (xmaportal.org). These data will be made public on publication.

Using DEM to Simulate Foot–Sediment Interaction. The open source software package LIGGGHTS (36, 37) was used to simulate a granular substrate. Validation simulations were carried out to determine the material properties required for simulating the poppy seeds. These validation experiments used a 10-cm^3 container 60% filled with poppy seeds (i.e., to a depth of 6 cm). In the first experiment, a metal ball (radius, 15 mm; density, 4,865 kg/m^3) was dropped from a height of 50 mm, and the depth of penetration was recorded. In the second experiment, the container was rotated 90° over a 2-s period to obtain the angle of repose. These experiments were then recreated in the DEM simulation using particles with a 0.5-mm radius (value obtained from measuring poppy seeds), and parameters were altered until simulations and experiments reasonably converged.

After the material parameters were determined, a 55-mm-deep, 180-mm-long, and 120-mm-wide virtual sediment box was constructed. This sediment box was constructed in the same virtual world space coordinates as in the XROMM Maya scene, and centered at and below the area in which the guineafowl foot contacted the poppy seeds. The sediment volume was sufficiently large to encompass all significant particle displacements, and thus to avoid major boundary effects. The virtual container was filled with particles of the same size and material properties as used in the validation tests. Particles were poured into the box and allowed to settle under gravity until at rest, and any particles located above the required height were deleted from the simulation.

The motion of each bone in the guineafowl limb was transferred to the discrete element simulation, using rigid cylinders as proxies for the limb elements (Fig. 2). Rigid cylinders provided the most parsimonious approach to representing the foot of the animal in this study; using the bone models would be entirely unsuitable, but attempting to use a more life-like representation of soft tissue without allowing for compliance (currently not computationally feasible) would be equally unrealistic.

Simulation data were visualized using Ovito (38) (ovito.org). The nature of the simulation is such that all particle velocities and displacements are recorded at each time step. Particles were assigned a value based on their initial starting location in the vertical dimension, essentially assigning particles to sedimentary layers that could be separated during visualization and observed independent of one another.

ACKNOWLEDGMENTS. We thank Robert Kambic and Beth Brainerd (Brown University) for assistance with experimental data collection and useful discussions during analysis; Dan Goldman, Mark Kingsbury, and Jeff Aguilar (Georgia Tech) for helpful advice and discussions about substrate choice; and Kate Wellspring (Beneski Museum of Natural History, Amherst College) for access to specimens. P.L.F. was supported by a Marie Curie International Outgoing Fellowship within the 7th European Framework Programme. XROMM analyses were supported by grants from the National Science Foundation (IOS-0925077 and DBI-0552051), the W.M. Keck Foundation, and the Bushnell Research and Education Fund (to S.M.G.). Simulations were carried out using High-End Computing Terascale Resource (Grant Q261856) and the Extreme Science and Engineering Discovery Environment (Grant TG-EAR130043) supercomputing resources.

1. Li C, Zhang T, Goldman DI (2013) A terradynamics of legged locomotion on granular media. *Science* 339(6126):1408–1412.
2. Maladen RD, Ding Y, Umbanhowar PB, Kamor A, Goldman DI (2011) Mechanical models of sandfish locomotion reveal principles of high-performance subsurface sand-swimming. *J R Soc Interface* 8(62):1332–4510.
3. Mazouchova N, Umbanhowar PB, Goldman DI (2013) Flipper-driven terrestrial locomotion of a sea turtle-inspired robot. *Bioinspir Biomim* 8(2):026007.
4. Stephens PA, Zaumyslova OY, Miquelle DG, Myslenkov AI, Hayward GD (2006) Estimating population density from indirect signs: Track counts and the Formozov–Malyshev–Pereleshin formula. *Anim Conserv* 9(3):339–348.
5. Mayle BA, Putman RJ, Wyllie I (2000) The use of trackway counts to establish an index of deer presence. *Mammal Rev* 30(3-4):233–237.
6. Brown R, Ferguson J, Lawrence M, Lees D (1987) *Tracks and Signs of the Birds of Britain and Europe* (Christopher Helm Publishing, London).
7. Castanera D, et al. (2013) Manus track preservation bias as a key factor for assessing trackmaker identity and quadrupedalism in basal ornithopods. *PLoS ONE* 8(1):e54177.
8. Clack J (1997) Devonian tetrapod trackways and trackmakers: A review of the fossils and footprints. *Palaeogeogr Palaeocl* 130:227–250.
9. Falkingham PL (2014) Interpreting ecology and behaviour from the vertebrate fossil track record. *J Zool* 292(4):222–228.
10. Falkingham PL, Bates KT, Margetts L, Manning PL (2011) The "Goldilocks" effect: Preservation bias in vertebrate track assemblages. *J R Soc Interface* 8(61):1142–1154.
11. Gatesy SM (2003) Direct and indirect track features: What sediment did a dinosaur touch? *Ichnos* 10:91–98.
12. Gatesy SM (2001) Skin impressions of Triassic theropods as records of foot movement. *Bull Museum Compar Zool* 156:137–149.
13. Thulborn RA (1990) *Dinosaur Tracks* (Chapman & Hall, London).
14. Thulborn RA, Wade M (1989) A Footprint as a History of Movement. *Dinosaur Tracks and Traces*, eds Gillette DD, Lockley MG (Cambridge Univ Press, Cambridge, UK), pp 51–56.
15. Allen JRL (1989) Fossil vertebrate tracks and indenter mechanics. *J Geol Soc London* 146:600–602.
16. Allen JRL (1997) Subfossil mammalian tracks (Flandrian) in the Severn Estuary, SW Britain: Mechanics of formation, preservation and distribution. *Philos Trans R Soc Lond B Biol Sci* 352:481–518.
17. Milàn J, Bromley RG (2006) True tracks, undertracks and eroded tracks: Experimental work with tetrapod tracks in laboratory and field. *Palaeogeogr Palaeoclimatol Palaeoecol* 231:253–264.
18. Milàn J, Bromley RG (2008) The impact of sediment consistency on track and undertrack morphology: Experiments with emu tracks in layered cement. *Ichnos* 15:19–27.

19. Manning PL (2004) A new approach to the analysis and interpretation of tracks: Examples from the dinosauria. *Geol Soc Lond Spec Publ* 228:93–123.
20. Ellis RG, Gatesy SM (2013) A biplanar X-ray method for three-dimensional analysis of track formation. *Palaeontologia Electronica* 16(1):1T.
21. Gould SJ (1977) *Ontogeny and Phylogeny* (Harvard Univ Press, Cambridge, MA).
22. Loope DB (2006) Dry-season tracks in dinosaur-triggered grainflows. *Palaios* 21: 132–142.
23. Loope DB (1986) Recognizing and utilizing vertebrate tracks in cross-section: Cenozoic hoofprints from Nebraska. *Palaios* 1:141–151.
24. Fornos JJ, Bromley RG, Clemmensen LB, Rodriguez-Perea A (2002) Tracks and trackways of *Myotragus balearicus* Bate (Artiodactyla, Caprinae) in Pleistocene aeolianites from Mallorca (Balearic Islands, Western Mediterranean). *Palaeogeogr Palaeoclimatol Palaeoecol* 180(4):277–313.
25. Padian K, Olsen PE (1984) The fossil trackway pteraichnus: Not pterosaurian, but crocodilian. *J Paleontol* 58:178–184.
26. Gatesy SM, Middleton KM, Jenkins FA, Shubin NH (1999) Three-dimensional preservation of foot movements in Triassic theropod dinosaurs. *Nature* 399:141–144.
27. Razzolini NL, et al. (2014) Intra-trackway morphological variations due to substrate consistency: The El Frontal dinosaur tracksite (Lower Cretaceous, Spain). *PLoS ONE* 9(4):e93708.
28. Farlow JO, et al. 2012 Dinosaur track sites of the Paluxy River Valley (Glen Rose Formation, Lower Cretaceous), Dinosaur Valley State Park, Somervell County, Texas. In *Proceedings of the V International Symposium about Dinosaur Palaeontology and their Environment*, pp 41–69, 10.1080/02724634.1988.10011689.
29. Padian K, Olsen PE (1984) Footprints of the Komodo monitor and the trackways of fossil reptiles. *Copeia* 1984(3):662–671.
30. Minter NJ, Braddy SJ, Davis RB (2007) Between a rock and a hard place: Arthropod trackways and ichnotaxonomy. *Lethaia* 40:365–375.
31. Kambic RE, Roberts TJ, Gatesy SM (2014) Long-axis rotation: A missing degree of freedom in avian bipedal locomotion. *J Exp Biol* 217(Pt 15):2770–2782.
32. Brainerd EL, et al. (2010) X-ray reconstruction of moving morphology (XROMM): Precision, accuracy and applications in comparative biomechanics research. *J Exp Zool A Ecol Genet Physiol* 313(5):262–279.
33. Gatesy SM, Baier DB, Jenkins FA, Dial KP (2010) Scientific rotoscoping: A morphology-based method of 3-D motion analysis and visualization. *J Exp Zool A Ecol Genet Physiol* 313(5):244–261.
34. Nyakatura JA, Fischer MS (2010) Functional morphology and three-dimensional kinematics of the thoraco-lumbar region of the spine of the two-toed sloth. *J Exp Biol* 213(Pt 24):4278–4290.
35. Baier DB, Gatesy SM, Dial KP (2013) Three-dimensional, high-resolution skeletal kinematics of the avian wing and shoulder during ascending flapping flight and uphill flap-running. *PLoS ONE* 8(5):e63982.
36. Kloss C, Goniva C; The Minerals, Metals & Materials Society (2011) LIGGGHTS: Open-source discrete element simulations of granular materials based on Lammps. In *Supplemental Proceedings: Materials Fabrication, Properties, Characterization, and Modeling* (Wiley, Hoboken, NJ), Vol. 2, pp. 781–788.
37. Kloss C, Goniva C, Hager A, Amberger S, Pirker S (2012) Models, algorithms and validation for opensource DEM and CFD-DEM. *Progr Computat Fluid Dynam* 12(2/3):140–152.
38. Stukowski A (2010) Visualization and analysis of atomistic simulation data with OVITO–the Open Visualization Tool. *Model Simul Mater Sci Eng* 18(1):015012.